THE GERONTOLOGICAL SOCIETY OF AMERICA®

Journals of Gerontology: Biological Sciences
cite as: *J Gerontol A Biol Sci Med Sci*, 2019, Vol. 74, No. 1, 33–43
doi:10.1093/gerona/gly198
Advance Access publication September 27, 2018

OXFORD

Original Article

The Rat Prefrontal-Cortex Transcriptome: Effects of Aging and Sporadic Alzheimer's Disease–Like Pathology

Natalia A. Stefanova, ScD,[1] Nikita I. Ershov, PhD,[1] Kseniya Yi Maksimova, PhD,[1,2] Natalia A. Muraleva, PhD,[1] Mikhail A. Tyumentsev, PhD,[1] and Nataliya G. Kolosova, ScD[1,3]

[1]Department of Molecular Mechanisms of Aging, Institute of Cytology and Genetics, Novosibirsk, Russia. [2]Department of Histology, Embryology and Cytology, Siberian State Medical University, Tomsk, Russia. [3]Department of Free Radical Chemistry, Novosibirsk State University, Russia.

Address correspondence to: Natalia A. Stefanova, ScD, Institute of Cytology and Genetics, Prospekt Lavrentyeva 10, Novosibirsk 630090, Russia. E-mail: stefanovan@mail.ru

Received: June 14, 2018; Editorial Decision Date: August 6, 2018

Decision Editor: Rozalyn Anderson, PhD

Abstract

Alzheimer's disease (AD) is the most widespread late-life dementia and involves the prefrontal cortex, a vulnerable brain region implicated in memory, emotion, cognition, and decision-making behavior. To understand the molecular differences between the effects of aging and AD on the prefrontal cortex, this study characterized the age-dependent changes in gene expression in Wistar rats (control) and OXYS rats (rodents that simulate key characteristics of sporadic AD) using RNA sequencing. We found that major altered biological processes during aging in Wistar rats were associated with immune processes. Gene expression changes during development of AD-like pathology as well as at the preclinical stage were related to neuronal plasticity, catalytic activity, lipid and immune processes, and mitochondria. A comparison of genes between data sets "OXYS rats" and "human AD" revealed similarity in expression alterations of genes related primarily to mitochondrial function; immune, endocrine, and circulatory systems; signal transduction; neuronal and synaptic processes; hypoxia; and apoptosis. Expression changes in mitochondrial processes identified in OXYS rats by RNA sequencing were confirmed by ultrastructural neuronal organelle alterations and low activity of respiratory chain complexes I, IV, and V in cortical mitochondria, suggesting that mitochondrial dysfunction appears to mediate or possibly even initiate the development of AD.

Keywords: RNA sequencing, Brain, Mitochondrial dysfunction, OXYS rats

Alzheimer's disease (AD) is the most widespread late-life dementia, currently without effective treatments (1,2). AD is characterized by accumulation of neurotoxic amyloid β peptide (Aβ), tau protein hyperphosphorylation, synaptic insufficiency, neuronal loss, inflammation, and mitochondrial dysfunction (3). The preclinical period of the disease and the role of Aβ in the initiation of clinical symptoms remain unclear even in rare early-onset familial form of AD, where accumulation of Aβ in the brain is caused by mutations in three separate genes: amyloid precursor protein (*APP*), presenilin 1 (*PSEN1*), and presenilin 2 (*PSEN2*) (4). Furthermore, in recent years, there is growing evidence that Aβ build up and tau protein accumulation are not a trigger but possibly downstream events in AD (5).

According to genome-wide association studies, the identified genetic risk factors for late-onset sporadic form of AD (the most prevalent form of the disease; ~95% of cases) can be subdivided into three overlapping groups/pathways (6): (a) cell-synaptic functioning (*BIN1*, *PICALM*, *CD33*, and *SORL1*), (b) immune system (*TREM2*, *CR1*, *CD33*, and *CLU*), and (c) genes related to lipid metabolism (*APOE*, *ABCA7*, and *CLU*). Nonetheless, direct interactions among these pathways remain unknown, as do their relation to Aβ accumulation, and what mechanisms are behind the primary neuronal dysfunction.

Aging is the primary risk factor for dementia (7,8), and age-related cognitive decline involves the prefrontal cortex, a vulnerable brain region implicated in memory, emotion, cognitive functions, decision making, and social behavior (9). Moreover, with age, there is increasing heterogeneity in the neuropathology underlying AD dementia (4). In the cases of sporadic form of AD, the disorder is driven by a complex interplay between numerous distinct genetic, epigenetic, and environmental factors (1,2). Growing data from brain imaging studies suggest that AD dementia appears only after

the addition of other pathological changes to a subthreshold level of AD pathology, in particular cerebrovascular dysfunction (4,10,11). It is clear that vascular deficits diminish the brain's supply of oxygen, energy, substrates, and nutrients and impair the clearance of Aβ. There is convincing evidence that mitochondria may mediate, drive, or contribute to these problems and a variety of AD-associated pathologies (12,13), but dissecting the details is still a major challenge for research on the disease pathogenesis.

In this study, we assessed the mechanisms of the development of AD-like pathology in senescence-accelerated OXYS rats. These animals spontaneously develop all key signs of AD such as structural neurodegenerative alterations, neuronal loss, synaptic damage, disturbances of the neurotrophic supply, cerebrovascular alterations, $A\beta_{1-42}$ accumulation and tau hyperphosphorylation in the hippocampus, and cognitive impairment (14–18). Recently, we have obtained convincing evidence that mitochondrial dysfunction can mediate or possibly initiate AD-like pathological molecular cascades in OXYS rats (19); however, we do not know the molecular genetic basis of the main cause of mitochondrial alterations.

Here, we performed a comparative gene expression analysis on the prefrontal cortex of Wistar rats (control) and OXYS rats to understand the molecular effects of aging and AD at different stages of the disease, including the preclinical stage, using RNA sequencing. In addition, were carried out comparisons with human AD data sets as well as electron microscopic analyses to evaluate neuronal alterations during the development of AD-like pathology in OXYS rats. Ultrastructural mitochondrial alterations were collated with the activity of respiratory chain complexes I, IV, and V in cortical mitochondria.

Methods

Animals

All the experimental procedures were in compliance with the European Communities Council Directive of 24 November 1986 (86/609/EEC). The protocol of the animal experiments was approved by the Commission on Bioethics of the Institute of Cytology and Genetics, Novosibirsk, Russia.

We used 20-day-old and 5- and 18-month-old male OXYS and Wistar rats (Novosibirsk, Russia). The OXYS strain was derived from the Wistar strain of rats as described earlier (20). The diets and living conditions of the animals as well as tissue sample preparation are shown in Supplementary Data 1.

Illumina Sequencing

More than 40 million single-end reads 50 bp long were obtained for each sample of cortical RNA, by Illumina nonstranded sequencing on an Illumina GAIIx instrument at the Genoanalitika Lab, Moscow, Russia (http://www.genoanalytica.ru/) in accordance with standard Illumina protocols (mRNA-Seq Sample Prep Kit). Briefly, polyadenylated mRNA was purified from total RNA using Sera-Mag Magnetic Oligo (dT) beads and then broken into small fragments by means of divalent cations and heating. Using a reverse transcriptase and random primers, we synthesized first- and second-strand cDNAs. The cDNA was processed in an end repair reaction with T4 DNA polymerase and Klenow DNA polymerase to blunt the termini. An "A" base was then added to the 3′ end of the blunt phosphorylated DNA fragments, and an Illumina adaptor with a single T overhang at its 3′ end was then ligated to the end of the DNA fragment, for hybridization in a single-read flow cell. After that, a size range of cDNA templates was selected, and these fragments were amplified on a cluster station using the Single-Read Cluster Generation Kit v2. Sequencing-by-synthesis (SBS) at 50-nucleotide length was performed by means of SBS v4 reagents on a Genome Analyzer IIx running the SCS2.8 software (Illumina).

Gene expression analysis was performed as described previously (18). The genes with p_{adj} less than .05 were selected as differentially expressed.

Comparisons With Previous Human AD Expression Studies

AD expression data from the NCBI SRA database under the accession number SRA060572 were analyzed. The data set is composed of four control and five AD cases from Emory University and three control and three AD cases from the University of Kentucky. The raw data were subjected to quality trimming and adapter removal and mapped to GRCh37 human genome assembly from the 1000 Genomes Project (www.internationalgenome.org), using TopHat v2.0.12 (21) and ENSEMBL GRCh37.82 gene annotation. Read counting and statistical analysis of differential expression were performed using the DESeq2 (22) R package. Given that the two data sets differ in both the source and sequencing protocol (single end vs paired end), a two-factor design (diagnosis and source of a data set) was applied. The genes with p_{adj} less than .05 were assumed to be differentially expressed. The one-to-one orthologous relationships between the *Homo sapiens* GRCh37 and *Rattus norvegicus* Rnor_5.0 gene annotations were extracted via the ENSEMBL BioMart web service (http://www.ensembl.org/biomart/martview) and used to compare the DEGs obtained for humans and rats.

Functional Analysis and Construction of Gene Interaction Networks

To identify the Gene Ontology (GO) terms overrepresented in a DEG list, the detected DEGs were subjected to functional enrichment analyses by means of the DAVID (http://david.abcc.ncifcrf.gov/summary.jsp) tool. Pathway analysis of the DEGs was conducted with WebGestalt GSAT (http://www.webgestalt.org/option.php) using the KEGG pathways (http://www.genome.jp/kegg/) and WikiPathways (https://www.wikipathways.org). The gene interaction networks were identified on the GeneMANIA web server (http://www.genemania.org/).

Electron Microscopic Examination

For this purpose, the prefrontal-cortex samples (n = 4) were prepared as described elsewhere (23). For evaluation of morphological features, neurons were identified in the electron micrographs (30 photos per animal). Next, all the morphological changes that are located in the neurons were painted in software. Ultrathin sections were examined under a JEOL JEM-100SX transmission electron microscope (JEOL Ltd, Japan) at 60 kV at the Interinstitutional Shared Center for Microscopic Analysis of Biological Objects (Institute of Cytology and Genetics, Novosibirsk, Russia). For quantitative analysis, electron-transparent regions were identified on the electron micrographs of cortical neurons and were painted using software. The photos were processed in Adobe Photoshop; for each photo, the following parameter was determined: the total area of each type of organelle located in the electron-transparent areas of the neurons. Then, the organelle-occupied proportion of the neuron area was calculated.

Assays of Activity of Mitochondrial Complexes I, IV, and V

Activities of these mitochondrial complexes were measured with enzyme assay kits (Abcam, Sigma-Aldrich, St. Louis, MO). Protein concentrations of mitochondrial lysates were estimated by means of the Bio-Rad Bradford Kit (Bio-Rad Laboratories, Hercules, CA). Enzymatic activities were measured spectrophotometrically on a CLARIOStar spectrophotometer (BMG Labtech, Germany) and expressed as changes of absorbance per minute per milligram of mitochondrial protein.

Statistical Analysis

The data were subjected to analysis of variance (ANOVA; Statistica 8.0 software). Two-way ANOVA was conducted to evaluate the age-dependent effects (age × genotype [strain]). The Newman–Keuls test was applied to significant main effects and interactions to assess the differences between some sets of means. The data were presented as mean ± *SEM*. The differences were considered statistically significant at p less than .05.

Results

Differential Expression of Genes in the Prefrontal Cortex of OXYS Rats

To identify the extent to which genes are differentially expressed in the prefrontal cortex in the period preceding the development (age 20 days), during manifestation (5 months), and at the well-pronounced stages (18 months) of the AD-like pathology in OXYS rats, gene expression was compared between OXYS rats and age-matched Wistar rats. We identified 292 protein-coding mRNAs ($p_{adj} < .05$) that are differentially expressed in 20-day-old OXYS rats. There were 424 DEGs at the age of 5 months and 1,405 DEGs at the age of 18 months (Figure 1A).

Among the 74 DEGs that matched among the three age periods (overlapping gene sets; Figure 1B), mRNA expression of 33 genes was increased and decreased for 40 genes in OXYS rats. Only the subunit of the pre-α-trypsin inhibitor complex (*Itih3*) involved in stabilization of the extracellular matrix was upregulated at the age of 20 days and downregulated at the ages of 5 and 18 months. Analysis of the 74 matching DEGs (among the three overlapping gene sets) using DAVID revealed two basic clusters that were related to "reproductive process" and "mitochondrion" (Supplementary Table 1). In addition, 22 from the 74 matching DEGs are among the top 30 DEGs for 18-month-old OXYS rats (Supplementary Figure 1). Note that in this list of top genes, there were all DEGs at the age of 5 months and 73.3% of DEGs at the age of 20 days, including NADH dehydrogenase ubiquinone 1 alpha subcomplex 10-like 1 (*Ndufa10l1*), a component of the respiratory chain Complex I, and 3-hydroxy-3-methylglutaryl-CoA synthase 2 (*Hmgcs2*), a control mitochondrial enzyme in ketogenesis, suggesting that impairment of mitochondrial function may precede the development of AD.

The most significant GO terms in 20-day-old OXYS rats were associated with nervous system development, catalytic activity, lipid and immune processes, and mitochondria. At the age of 5 months, GO terms were also associated with nervous system development, immune and lipid processes, catalytic activity, and protein binding. In 18-month-old OXYS rats, highlighted GO terms were associated with regulation of cell communication and signal transduction, nervous system development, regulation of cell death, response to oxygen levels, ion binding, catalytic activity, gliogenesis, synaptic processes, and mitochondria (Figure 1C).

According to the analyses of KEGG and Wiki pathways ($p <$ .01), in 20-day-old OXYS rats, genes of sphingolipid metabolism were upregulated or downregulated; MAPK- and Hedgehog signaling pathways, phagosome, and gap junction were upregulated (Figure 1D). At the age of 5 months, the pathways involved in lipid metabolism, cellular community, cell death and circulatory system were upregulated, and the pathways associated with catabolism and the immune system were downregulated. We highlighted among the top pathways in 18-month-old OXYS rats the following categories: genes of immune processes were upregulated or downregulated; autophagy, adipogenesis, and signal transduction were upregulated; genes associated with neurodegenerative diseases such as AD, Parkinson's disease, and Huntington's disease were downregulated (Figure 1D).

Age-Associated Prefrontal-Cortex Transcriptome Changes in OXYS and Wistar Rats

We found that in OXYS rats, 6,618 genes significantly changed expression between the ages of 20 days and 5 months, and 5,686 genes changed expression between the ages of 5 and 18 months. In Wistar rats, 5,727 genes significantly changed expression between the ages of 20 days and 5 months, and 97 genes changed expression levels between the ages of 5 and 18 months (Figure 2A–C).

To determine the functional gene changes that occur throughout the life span and during the development of AD-like pathology, we performed the KEGG and Wiki pathway analyses ($p <$ .01). We found that in both rat strains by the age of 5 months, the annotated pathways in almost all cases were similar. Between the top 30 significant pathways ($p_{adj} <$ 8e–08) identified in OXYS rats and the top 30 significant pathways ($p_{adj} <$ 8e–08) identified in Wistar rats (Supplementary Tables 2 and 3), the matching pathways are related to synaptic and immune processes, adipogenesis, the cell cycle, focal adhesion, and signal transduction.

As for the age period between 5 and 18 months, in Wistar rats, the DEGs were associated with immune processes and phagosomes (Supplementary Table 4). In contrast, in OXYS rats, progression of AD-like pathology was associated with a large number of signaling pathways. Among the most significant pathways ($p_{adj} <$ 5e–06), the DEGs were associated with energy- and lipid-related metabolic pathways; signal transduction; cell death; immune, endocrine and circulatory systems; neuronal processes; and neurodegenerative diseases such as AD, Parkinson's disease, and Huntington's disease (Figure 2D; Supplementary Table 5).

We next analyzed the 67 DEGs in OXYS rats related to the AD pathway according to KEGG pathway analysis (Supplementary Table 6; Supplementary Figure 2). The expression levels of genes involved in the processing of Aβ precursor protein (*Apbb1*, amyloid β precursor protein–binding family B member 1) and γ-secretase (*Psen2*, presenilin 2, and *Aph1a*, aph-1 homolog A, gamma-secretase subunit) were high. The expression levels of genes related to α-secretase (*Adam10*, ADAM metallopeptidase domain 10, and *Adam17*, ADAM metallopeptidase domain 1), APP-BP (*Nae1*, NEDD8 activating enzyme E1 subunit 1), aggregation of Aβ (*Lpl*, lipoprotein lipase), and degradation of Aβ (*Mme*, membrane metalloendopeptidase) were low. In addition, according to DAVID, changes in gene expression were related to mitochondrial functions, synaptic processes, kinase activity (in particular, tau protein kinase activity), responses to hypoxia and oxidative stress, and apoptosis (Supplementary Table 6).

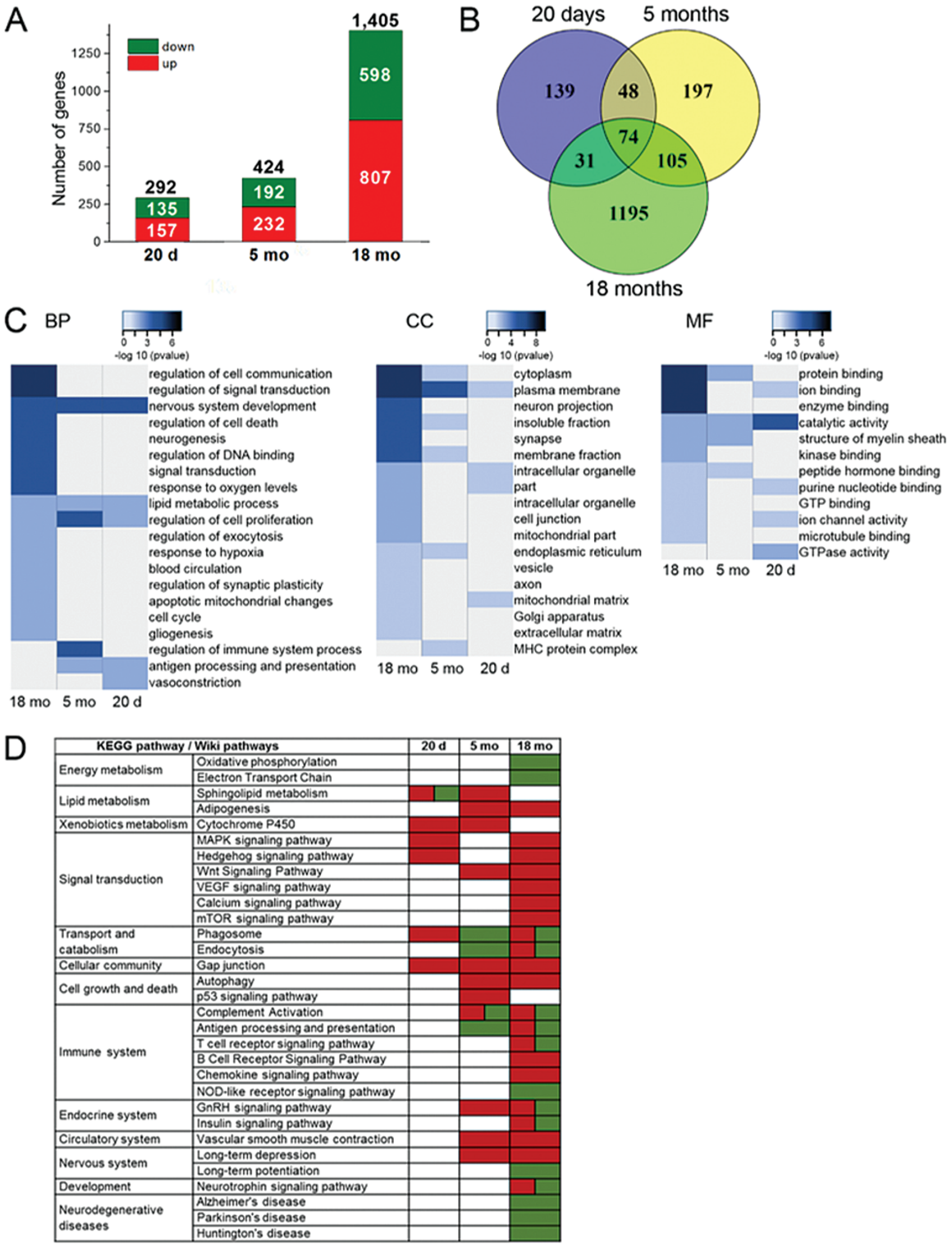

Figure 1. Differential expression of genes: the effect of genotype. (**A**) The number of DEGs in the prefrontal cortex of 20-d-old and 5- and 18-mo-old OXYS rats compared with age-matched Wistar rats. (**B**) Venn diagram shows overlapping sets of DEGs in OXYS rats compared with Wistar rats. (**C**) Gene Ontology terms (BP = biological processes; CC = cellular component; MF = molecular function) in OXYS rats according to DAVID. (**D**) Pathways (according to KEGG), which undergo changes in OXYS rats, when compared with age-matched Wistar rats. Pathways are marked in red if upregulated and green if downregulated.

Comparison of Human and OXYS Rats' AD-Like Brain Transcriptomes

To confirm our previous findings (14–19) and the results obtained in this study indicating that OXYS rats are a suitable model for studying the initiation and progression of pathological molecular cascades of AD, human AD prefrontal-cortex transcriptome data sets were analyzed. Analysis of DEGs resulted in identification of 1,733 DEGs in human AD (p_{adj} < .05), which were next compared with 1,418 DEGs identified for OXYS rats at the well-pronounced stage (age 18 months) of AD (Figure 3A). This comparison revealed an overlap

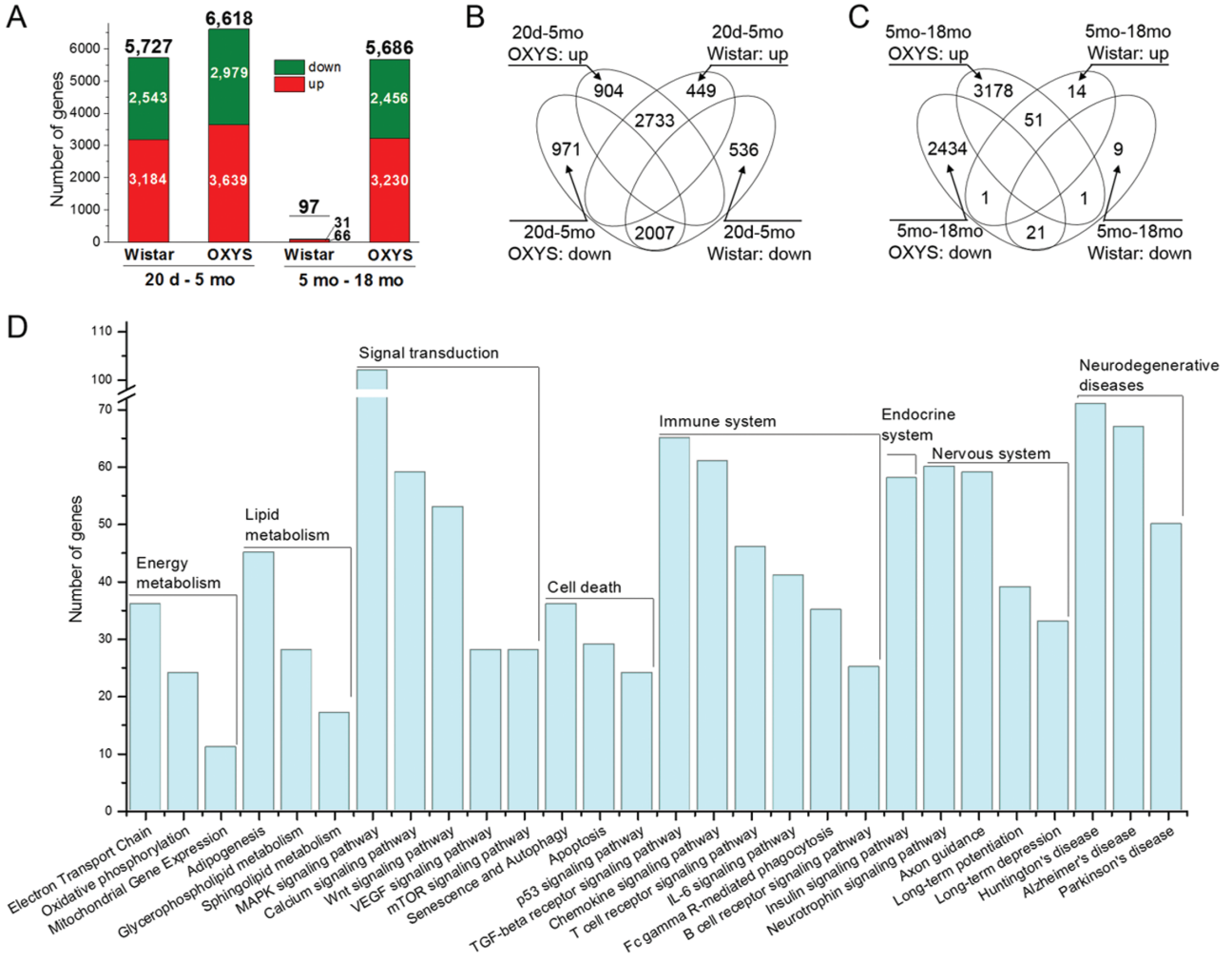

Figure 2. Differential expression of genes: the effect of age. (**A**) The number of genes that change expression with age in the prefrontal cortex of OXYS and Wistar rats. Venn diagrams show overlapping sets of genes that change expression in OXYS and Wistar rats (**B**) from the age of 20 d to 5 mo and (**C**) from the age of 5–18 mo. (**D**) Pathways (according to KEGG and Wiki), which undergo changes in OXYS rats from the age of 5–18 mo.

consisting of 135 genes, including 73 DEGs with unidirectional gene expression (Figure 3B). According to DAVID, these 73 matching DEGs are related to neuronal and synaptic processes (Figure 3C). We next constructed the interaction network for these DEGs by means of GeneMANIA (Supplementary Figure 3). We found that despite the small number of DEGs related to GO terms, the most enriched of them were associated with mitochondrial functions. It is noteworthy that among the 73 matching DEGs, 12 genes (*BNIP3*, *KRAS*, *CHDH*, *CHCHD7*, *CDKL2*, *DLD*, *GDAP1*, *GLRX2*, *GLRX3*, *LPIN1*, *MTCH2*, and *SUCLA2*) were directly or indirectly associated with mitochondrial processes, according to DAVID analyses (Supplementary Table 7).

Common altered biological processes between human AD and OXYS rats

To further compare human and OXYS rats' AD-like brain transcriptomes, GO terms of DAVID and KEGG analyses were used. GO analysis revealed that upregulated genes for humans were the most significantly ($p < .0001$) associated with regulation of cell death, response to wounding, and an inflammatory response. In OXYS rats, upregulated genes were the most significantly ($p < .0001$) associated with a response to oxygen levels, neuron development, a response to hypoxia, blood circulation, synapse, and ion binding. Downregulated genes in OXYS rats were significantly enriched in cell cycle processes, GTPase activity, and nuclear processes ($p < .01$). In human AD, the downregulated genes were mainly associated with synaptic processes, ion transport, and ATPase activity ($p < .0001$). Common upregulated biological processes between humans and OXYS rats included regulation of cell death, an intracellular signaling cascade, a response to hypoxia, cell proliferation, extracellular matrix, and protein binding ($p < .05$). Similar to human AD, OXYS rats show a decline of a protein catabolic process, nucleotide binding, GTPase activity, and mitochondrial processes ($p < .05$; Supplementary Table 8).

KEGG analyses revealed an overlap consisting of 52% signaling pathways ($p < .05$) between human AD and OXYS rats; the majority of these pathways were related to nucleotide metabolism; endocytosis; lysosomes; the cell cycle; apoptosis; cellular community; immune, endocrine, and circulatory systems; signal transduction; and neuronal and synaptic processes (Supplementary Table 9; Figure 3D).

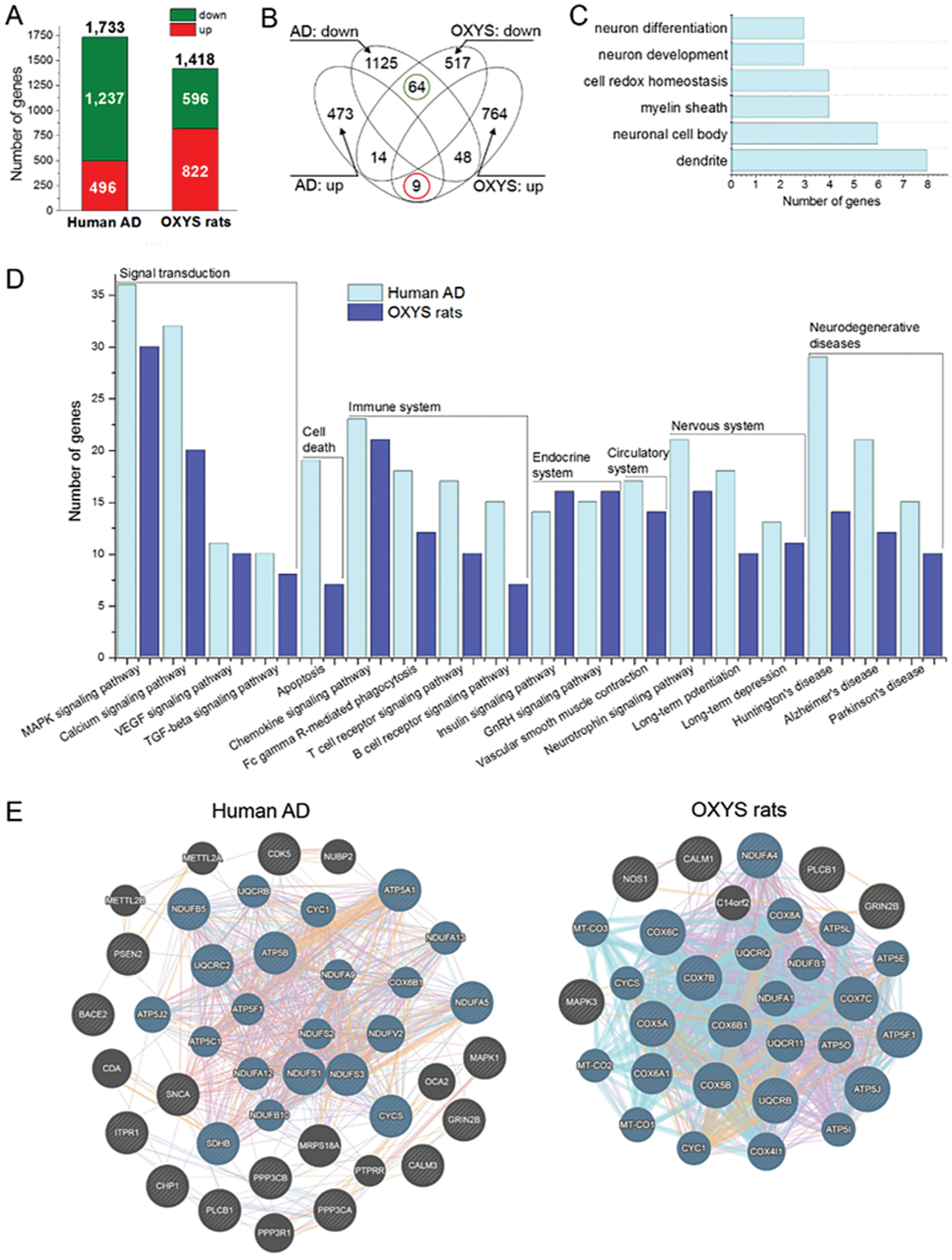

Figure 3. Differential expression of genes: a comparison of human AD and OXYS rats. (**A**)The number of DEGs in the prefrontal cortex of human AD and OXYS rats. (**B**) A Venn diagram shows overlapping sets of DEGs in human AD and OXYS rats. (**C**) Gene Ontology (GO) terms for the 73 DEGs common for human AD and OXYS rats. (**D**) Pathways (according to KEGG) in the overlap between human AD and OXYS rats. (**E**) Interaction networks for the DEGs in human and OXYS rats involved in the AD pathway. The most enriched GO term in both groups was related to the respiratory electron transport chain (blue circles).

In addition, pathways related to neurodegenerative diseases such as AD, Parkinson's disease, and Huntington's disease matched between human AD and OXYS rats (Figure 3D). Using GeneMANIA, we next constructed the interaction networks for the DEGs in humans (21 genes, p_{adj} = 1.64e−05) and OXYS rats (12 genes, p_{adj} = 0.01) involved in the AD metabolic pathway (Figure 3E). We

found that almost all the GO terms enriched in humans and OXYS rats were related to mitochondrial functions. The most enriched GO term in both groups was related to the respiratory electron transport chain ($p < 4.78e{-}34$ for human AD and $p < 2.08e{-}51$ for OXYS rats; Supplementary Table 10). When we compared the DEGs that are associated with AD, Parkinson's disease, and Huntington's disease, we found that matching DEGs in humans (nine genes) and matching DEGs in OXYS rats (seven genes) were mostly related to complexes I, IV, and V of the electron transport chain (Supplementary Figure 4). These findings support the hypothesis that mitochondrial dysfunction may be a trigger for the development of neurodegenerative diseases.

Age-dependent changes in the expression of the genes matching between human AD and OXYS rats

Because significant similarities in alterations of gene expression were found in the prefrontal cortex of OXYS rats at the advanced stage of the disease and in patients with AD, we next determined which genes from the matching 73 DEGs changed expression with age in OXYS rats (Supplementary Table 11). Among these AD-related genes, the expression of the important for synaptic processes serine protease 12 (Prss12) (24) significantly decreased in OXYS rats at all stages of disease including the preclinical period (age 20 days). In addition, we highlighted six genes (*Fam129a*, *Slc7a14*, *Ppp1r3b*, *Vwc2l*, *Xrcc6*, and *Ctxn3*) that are differentially expressed in OXYS rats already at the early stage (age 5 months) of AD. The expression of *Fam129a*, which encodes a protein called "family with sequence similarity 129 member A" and is involved in regulating p53-mediated apoptosis (25) was twofold higher both in OXYS rats and in human AD. Protein phosphatase 1 regulatory subunit 3B (Ppp1r3b), which is involved in lipid metabolism and considered a candidate gene of AD (26), was also upregulated in OXYS rats and human AD. Among the four downregulated genes, cortexin 3 (*Ctxn3*) showed the most significantly changed expression. Recently, it was suggested that overexpression of CTXN3 may lead to a decrease in Aβ peptide production by directly modulating APP metabolism (27).

Major Altered Biological Processes During Aging and Development of AD-Like Pathology

To determine which processes play more important roles (ie, are enriched) in OXYS and in Wistar rats between two age periods, we next performed functional annotation clustering with DAVID for DEGs exclusively expressed in each rat strain (Supplementary Table 12). In OXYS rats, between the ages of 20 days and 5 months, 904 genes exclusively showing upregulated expression (Figure 2B) were mainly related to a protein catabolic process, protein folding, proteasome activity, a cellular response to stress, the cell cycle, ion binding, and antigen processing and presentation. The 971 genes exclusively downregulated in OXYS rats were related to ATP binding, GTPase activity, and synaptic and neuronal processes. In Wistar rats during the same period, there were 449 genes that showed exclusively upregulated expression (Figure 2B); they were mainly related to a response to an abiotic stimulus, cytoskeleton, and a lipid process. The 536 exclusively downregulated genes were related to tube development and the extracellular matrix.

In OXYS rats, between the ages of 5 and 18 months, 3,178 genes that were exclusively upregulated and 2,434 genes that were exclusively downregulated (Figure 2C) were associated with a big number of significant clusters by DAVID. Among the 10 most significant clusters, the upregulated processes were related to synaptic and neuronal processes, mitochondria, ATP binding, enzyme binding, and protein transport (Supplementary Table 12). The genes downregulated in OXYS rats were related to nucleoplasm, a ubiquitin-dependent protein catabolic process, intracellular transport, ion binding, enzyme binding, and transcription (Supplementary Table 12). In Wistar rats during the same period, there were only 14 and 9 genes that were exclusively upregulated and downregulated, respectively (Figure 2C). Only upregulated genes were associated with two clusters related to cell activation (Supplementary Table 12).

For a more complete understanding of which processes make the most significant contribution to the development and progression of AD-like pathology and their chronological sequence, we next compared the GO terms for exclusively upregulated and downregulated DEGs between the two age periods in OXYS rats. By the age of manifestation of disease-like pathology (age 5 months), the exclusively upregulated processes mainly were related to immune functions and protein folding; the exclusively downregulated processes were mainly related to a lipid process (Figure 4). By the age of the well-pronounced stage (age 18 months) of AD in OXYS rats, the exclusively upregulated processes mainly were related to synaptic processes and mitochondria, and the downregulated processes were related to protein import, cell–cell signaling, and an energy metabolic process (Figure 4). The processes related to cell death, synaptic and neuronal processes, ion channel activity, and mitochondria were upregulated or downregulated in OXYS rats by the age of 18 months. During both age periods, the upregulated GO terms were associated with regulation of biological processes and mitochondria; downregulated GO terms were associated with mitosis, nuclear division, and organelle fission (Figure 4). The processes related to protein localization, the Golgi apparatus, ion binding, enzyme binding, a response to DNA damage stimulus, and synaptic functions were upregulated or downregulated in OXYS rats for both age periods. The processes that were upregulated by the age of 5 months and then were downregulated by the age of 18 months were mainly associated with nuclear processes. Conversely, the processes that were downregulated by the age of

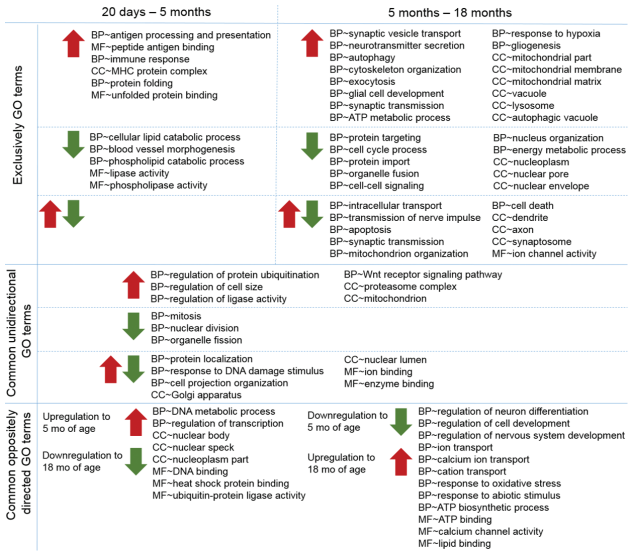

Figure 4. The Gene Ontology (GO) terms according to DAVID for exclusively upregulated and downregulated DEGs between two age periods in OXYS rats. BP = biological processes; MF = molecular functions; and CC = cellular components.

5 months and then were upregulated by the age of 18 months were mainly associated with regulation of neuronal development, ion transport, and ATP binding (Figure 4).

Mitochondrial Alterations in OXYS Rats

Here, we found that already at the preclinical stage, OXYS rats showed changes in gene expression related to mitochondrial function. Therefore, we next examined ultrastructural characteristics of the mitochondrial apparatus in the neurons of the prefrontal cortex of OXYS and Wistar rats at 20 days and at 5 and 18 months of age (Figure 5A–F). In 20-day-old OXYS rats, the state of mitochondrial ultrastructure in cortical neurons was comparable to that of Wistar rats with only occasional and modest disruption of ultrastructural features. In contrast, by the age of 5 months, some neuronal mitochondria of OXYS rats manifested considerable disorganization of cristae structure, matrix rarefication, and disordered membrane architecture. In 18-month-old OXYS rats, these changes were even more pronounced, with a lucid matrix, widespread membrane disorganization, broken and scarce cristae, and swollen mitochondria.

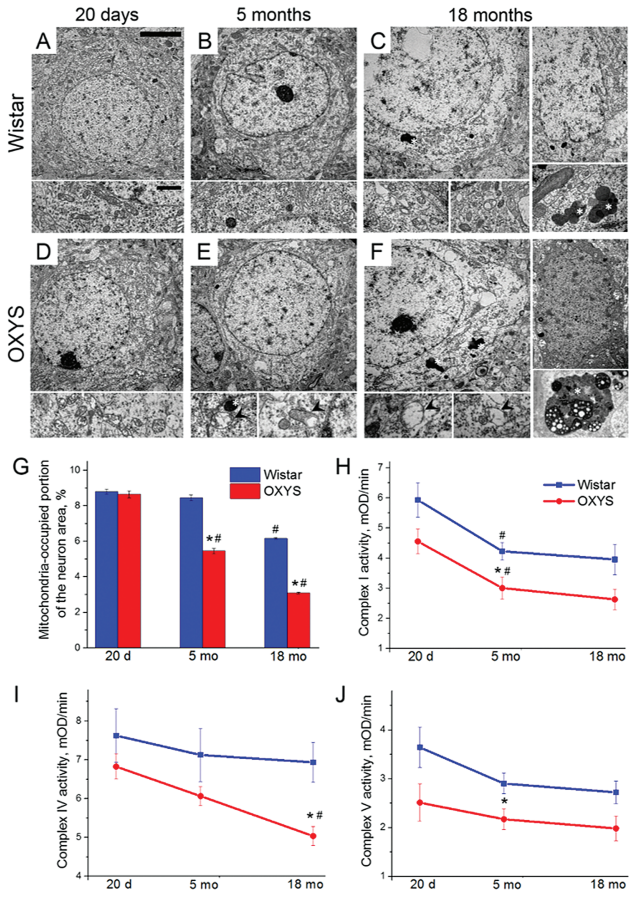

Figure 5. Cortical neurons of both Wistar (**A–C**) and OXYS (**D–F**) rats show age-related deterioration of mitochondrial structure, which is more prominent in OXYS rats. Scale bar = 4 μm. High-magnification pictures of Wistar and OXYS mitochondria show organelles with a rarefied matrix and broken cristae (black arrowheads). Lipofuscin accumulation (white asterisks) is also evident: more prominently in OXYS rats, especially in 18-mo-old animals. Scale bar = 1 μm. (**G**) The mitochondria-occupied portion of the cortical neuron area in OXYS and Wistar rats. The activities of respiratory chain complexes I (**H**), IV (**I**), and V (**J**) in the mitochondria of the prefrontal cortex of Wistar and OXYS rats. *Significant differences between the strains of the same age; #significant differences with the previous age within the strain. OD = optical density.

The results were quantified by stereotypic methods. For each of the three age groups of OXYS and Wistar rats, we calculated the portion occupied by mitochondria, lysosomes, Golgi apparatus, endoplasmic reticulum, vacuoles, of by lipofuscin (Supplementary Table 13) of the whole neuron area. We found that the mitochondria-occupied portion did not differ between the two rat strains at the age of 20 days and decreased in OXYS rats from the age of 5 months (Figure 5G). In addition, already at the age of 20 days, in OXYS rats, the specific areas of lysosomes and vacuoles were greater, and the specific area of the Golgi complex was smaller in comparison with Wistar rats ($p < .05$; Supplementary Table 13). At the age of 5 months in OXYS rats, the specific areas of the endoplasmic reticulum and Golgi complex were smaller, and those of vacuoles and lipofuscin were greater when compared with Wistar rats ($p < .05$). With age, these differences progressed: in 18-month-old OXYS rats, the specific area of lipofuscin, lysosomes, and vacuoles was 1.7-fold, 1.6-fold, and 1.4-fold greater, respectively, and that of the endoplasmic reticulum and Golgi complex was smaller in comparison with Wistar rats ($p < .05$; Supplementary Table 13).

A decrease in the activity of the respiratory chain is an important sign of the impairment of mitochondrial function in the AD brain. Finally, we have measured age-related changes in the activities of the respiratory chain complexes I, IV, and V in the mitochondria of the prefrontal cortex of Wistar and OXYS rats. According to ANOVA, the activity of complexes I, IV, and V was lower in OXYS rats ($F_{1,36} = 14.6$, $p = .001$; $F_{1,36} = 9.8$, $p = .0047$; and $F_{1,40} = 14.01$, $p = .00057$, respectively) with the interstrain difference being significant at the age of 5 months ($p < .05$) for complexes I and V and at the age of 18 months for complex IV ($p < .05$; Figure 5H–J).

Discussion

The dementia of AD is diagnosed when an individual loses independent functioning as a result of impairments in cognitive function (28). These symptoms are thought to be a direct reflection of the accrual of pathological alterations in multiple brain regions related to memory, for example, the prefrontal cortex. Transcriptomic analyses, which imply no a priori etiological hypotheses, show much promise for elucidating the pathogenesis of complex diseases including AD (29). Because in humans, such studies (especially those on the early asymptomatic stages of AD) are problematic, in the present study, we used OXYS rats to understand the molecular aberrations that lead to AD-like pathology. We found that most of DEGs in the prefrontal cortex during the development of AD-like pathology as well as genes at the preclinical stage are related to specific molecular processes such as neuronal plasticity, catalytic activity, lipid metabolic processes, immune processes, and mitochondrial function.

The onset of adolescence and adulthood triggers significant changes in gene expression as does the onset of old age. Between the ages of 20 days and 5 months, there were changes in the expression of more than 5,500 genes in Wistar rats and OXYS rats. Accordingly, the altered pathways matching between the two rat strains in this age period are related to neurotrophic supplementation and synaptic plasticity, immune and lipid processes, cell cycle, and signal pathways such as MAPK and calcium pathways. With age (from 5 to 18 months) in Wistar rats, only 97 genes changed their expression; most of them are related to immune processes. In OXYS rats, in the course of progression of AD-like pathology expression of more

than 5,500 genes underwent changes. Most of them are related to neuronal and synaptic plasticity; immune, endocrine, and circulatory systems; mitochondrial function; and cell death.

The progression of AD-like pathology in OXYS rats occurs during the changes in the expression of 67 genes that are associated with the AD metabolic pathway and could play an important role in the pathogenesis of the disease. These DEGs are mainly related to APP and Aβ processing, regulation of tau protein, mitochondrial function, and synaptic processes. It is worth noting that the increases in the amounts of APP, $A\beta_{1-42}$, and extracellular Aβ deposits in the brain of 12-month-old OXYS rats occur later than do mitochondrial function abnormalities, hyperphosphorylation of the tau protein, synaptic loss, and neuronal cell death (14,15,30). Increasing evidence points to a role of mitochondrial alterations upstream of Aβ and tau aberrations in AD (31). Indeed, in this study in the prefrontal cortex, and recently, in the hippocampus (19), we found that already at the preclinical stage, OXYS rats manifested some characteristic ultrastructural changes and decreased activity of respiratory complexes I, IV, and V, as well as the changes in the expression of genes related to mitochondrial function; these alterations progressed with the development of AD-like pathology. It is noteworthy that although there is a decrease in mitochondrial function with aging in OXYS rats, there is an increase in the expression of many mitochondrial genes. The consequence of mitochondrial dysfunction is suppression of energy-consuming processes in neurons, inflammation, disruption of synaptic plasticity, and, ultimately, neuronal death (31).

The neurodegenerative changes in the brain of OXYS rats take place simultaneously with formation of demyelination foci (increasing with age) (32) and structural changes in microtubules (23), which could be a consequence of the hyperphosphorylation of tau protein (14,15). At the well-pronounced stages of AD in OXYS rats, the neurotoxic effect of tau protein may also be mediated by Aβ, which enhances tau phosphorylation through the activation of Cdk5 and GSK3b kinases, caspases 3 and 9, and calpain (33). Here, we found that progression of the signs of AD in OXYS rats occurs with a decrease in the level of mRNA of *Gsk3b* ($\log_2$FC = –0.26) and an increase in the level of *Cdk5* ($\log_2$FC = 0.32), *Casp9* ($\log_2$FC = 0.32), and *Capn1* ($\log_2$FC = 0.4) in the prefrontal cortex (where FC is fold change).

There is growing evidence that pathological accumulation of Aβ is obviously due not so much to overproduction of APP, as to an imbalance in the production and clearance of Aβ (34). The increased accumulation of Aβ with age in the brain of OXYS rats (15), along with an increase of expression of genes involved in the processing of APP (*Apbb1*, *Psen2*, and *Aph1a*) may be associated with disturbances in degradation processes. Indirectly, this finding indicates a decrease in the expression of genes involved in aggregation of Aβ (*Lpl*) and its degradation (*Mme*). Downregulation of MME causes accumulation of Aβ in the brain (35).

A comparison of genes in OXYS rats and human AD data sets revealed similarities in alterations of expression of 73 genes related primarily to mitochondrial function and neuronal and synaptic processes. In addition, between humans and rats, there were common pathways related to neurodegenerative diseases such as AD, Parkinson's disease, and Huntington's disease. The matching genes among the overlapping gene sets of these neurodegenerative diseases were found to be related to the electron transport chain, thus supporting the hypothesis that mitochondrial dysfunction may be a trigger of the development of neurodegenerative processes (31). Our results revealed age-dependent changes in the structural organization of cellular organelles, including mitochondria, in the neurons of the prefrontal cortex of OXYS rats. In addition, an increase in the relative proportion of lysosomes and vacuoles in OXYS rats already at the age of 20 days can be considered an enhancement of autophagy and apoptosis. After birth, the high activity of cerebral apoptosis related to the formation of interneuronal contacts and elimination of "transitional" cell populations (36) as well as neurogenesis are suggestive of enhanced reactive oxygen species production (37). It was this age period when increased reactive oxygen species production (19) and accumulation of deletions in mitochondrial DNA (38) have been detected in the brain of OXYS rats.

In addition, significantly altered biological processes in the prefrontal cortex both during human AD and in OXYS rats were found here to be related to immune, endocrine, and circulatory systems and to signal transduction. A transcriptomic profile of expression of genes related to immune processes in both the prefrontal cortex and retina (39) of old OXYS rats may be described as defective inflammation. In particular, the changes in the expression of genes involved in gliogenesis in the prefrontal cortex of OXYS rats are indicative of the increased proliferation of glial cells with age. Recently, we reported the activation of proliferation of glial cells in the hippocampus of 18-month-old OXYS rats that contributes to the neuroinflammatory processes associated with AD-like pathology (23). Nonetheless, the alterations in the structure of microglial cells (changes that are characteristic of aging) in the hippocampus of OXYS rats (23) reflect the loss of their regulatory functions related to migration, clearance of cellular waste, and, ultimately, neuronal survival (40). We assume that a systemic immune imbalance (23,41–45) may create a certain metabolic background for the development of many manifestations of accelerated aging in OXYS rats, including AD-like pathology.

Another finding in our study is the differential expression of genes related to the hypoxia response, as well as genes involved in the circulatory system. Recently, we showed that in the hippocampus of OXYS rats, transcriptomic changes in the expression of genes functionally associated with cerebrovascular processes occurred already in the early period of life (18). With age, when AD-like pathology progresses, OXYS rats develop structural and functional alterations in the cerebral blood flow typical of chronic ischemia (46,47). The increased APP production and Aβ accumulation in the brain of OXYS rats (14,15) may also be involved in cerebrovascular dysfunction; brain ischemia activates cleavage of APP by β- and γ-secretases (48). Moreover, cerebrovascular dysfunction is considered a major risk factor of AD, which precedes and facilitates the launch of a neurodegenerative process, and chronic ischemia inevitably contributes to the progression of neurodegenerative changes (49).

On the basis of our present and recent results, we can conclude that mitochondrial impairments in OXYS rats are the earliest change in the development of AD-like pathology and progress with age along with the age-related lipid and immune aberrations, cerebrovascular alterations, and increased neuronal degeneration. In conclusion, our study presents RNA-seq analysis yielding a more detailed picture of transcriptional changes with age to understand the molecular mechanisms of brain aging and AD.

Supplementary Material

Supplementary data is available at *The Journals of Gerontology, Series A: Biological Sciences and Medical Sciences* online.

Funding

This work was supported by a Russian Scientific Foundation grant (16-15-10005) and partly (the electron microscopic analysis) by a grant from the Russian Foundation for Basic Research (18-015-00320).

Conflict of Interest

None reported.

References

1. Frere S, Slutsky I. Alzheimer's disease: from firing instability to homeostasis network collapse. *Neuron*. 2018;97:32–58. doi:10.1016/j.neuron.2017.11.028
2. Zhou L, Verstreken P. Reprogramming neurodegeneration in the big data era. *Curr Opin Neurobiol*. 2018;48:167–173. doi:10.1016/j.conb.2017.12.015
3. Querfurth HW, LaFerla FM. Alzheimer's disease. *N Engl J Med*. 2010;362:329–344. doi:10.1056/NEJMra0909142
4. Bondi MW, Edmonds EC, Salmon DP. Alzheimer's disease: past, present, and future. *J Int Neuropsychol Soc*. 2017;23:818–831. doi:10.1017/S135561771700100X
5. Drachman DA. The amyloid hypothesis, time to move on: amyloid is the downstream result, not cause, of Alzheimer's disease. *Alzheimers Dement*. 2014;10:372–380. doi:10.1016/j.jalz.2013.11.003
6. Jones L, Holmans PA, Hamshere ML, et al. Genetic evidence implicates the immune system and cholesterol metabolism in the aetiology of Alzheimer's disease. *PLoS One*. 2010;5:e13950. doi:10.1371/journal.pone.0013950
7. Lin CH, Lin E, Lane HY. Genetic biomarkers on age-related cognitive decline. *Front Psychiatry*. 2017;8:247. doi:10.3389/fpsyt.2017.00247
8. Pereira AC, Gray JD, Kogan JF, et al. Age and Alzheimer's disease gene expression profiles reversed by the glutamate modulator riluzole. *Mol Psychiatry*. 2017;22:296–305. doi:10.1038/mp.2016.33
9. Zhong S, Zhang S, Fan X, et al. A single-cell RNA-seq survey of the developmental landscape of the human prefrontal cortex. *Nature*. 2018;555:524–528. doi:10.1038/nature25980
10. de la Torre JC. Vascular risk factor detection and control may prevent Alzheimer's disease. *Ageing Res Rev*. 2010;9:218–225. doi:10.1016/j.arr.2010.04.002
11. Tarantini S, Tran CHT, Gordon GR, Ungvari Z, Csiszar A. Impaired neurovascular coupling in aging and Alzheimer's disease: contribution of astrocyte dysfunction and endothelial impairment to cognitive decline. *Exp Gerontol*. 2017;94:52–58. doi:10.1016/j.exger.2016.11.004
12. Swerdlow RH, Koppel S, Weidling I, Hayley C, Ji Y, Wilkins HM. Mitochondria, cybrids, aging, and Alzheimer's disease. *Prog Mol Biol Transl Sci*. 2017;146:259–302. doi:10.1016/bs.pmbts.2016.12.017
13. Theurey P, Pizzo P. The aging mitochondria. *Genes (Basel)*. 2018;9:E22. doi:10.3390/genes9010022
14. Stefanova NA, Kozhevnikova OS, Vitovtov AO, et al. Senescence-accelerated OXYS rats: a model of age-related cognitive decline with relevance to abnormalities in Alzheimer disease. *Cell Cycle*. 2014;13:898–909. doi:10.4161/cc.28255
15. Stefanova NA, Muraleva NA, Korbolina EE, Kiseleva E, Maksimova KY, Kolosova NG. Amyloid accumulation is a late event in sporadic Alzheimer's disease-like pathology in nontransgenic rats. *Oncotarget*. 2015;6:1396–1413. doi:10.18632/oncotarget.2751
16. Stefanova NA, Muraleva NA, Maksimova KY, et al. An antioxidant specifically targeting mitochondria delays progression of Alzheimer's disease-like pathology. *Aging (Albany NY)*. 2016;8:2713–2733. doi:10.18632/aging.101054
17. Rudnitskaya EA, Kolosova NG, Stefanova NA. Impact of changes in neurotrophic supplementation on development of Alzheimer's disease-like pathology in oxys rats. *Biochemistry (Mosc)*. 2017;82:318–329. doi:10.1134/S0006297917030105
18. Stefanova NA, Maksimova KY, Rudnitskaya EA, Muraleva NA, Kolosova NG. Association of cerebrovascular dysfunction with the development of Alzheimer's disease-like pathology in OXYS rats. *BMC Genomics*. 2018;19 (Suppl 3):75. doi:10.1186/s12864-018-4480-9
19. Tyumentsev MA, Stefanova NA, Muraleva NA, et al. Mitochondrial dysfunction as a predictor and driver of Alzheimer's disease-like pathology in OXYS rats. *J Alzheimers Dis*. 2018;63:1075–1088. doi:10.3233/JAD-180065
20. Stefanova NA, Fursova AZ, Kolosova NG. Behavioral effects induced by mitochondria-targeted antioxidant SkQ1 in Wistar and senescence-accelerated OXYS rats. *J Alzheimers Dis*. 2010;21:479–491. doi:10.3233/JAD-2010-091675
21. Kim D, Pertea G, Trapnell C, Pimentel H, Kelley R, Salzberg SL. TopHat2: accurate alignment of transcriptomes in the presence of insertions, deletions and gene fusions. *Genome Biol*. 2013;14:R36. doi:10.1186/gb-2013-14-4-r36
22. Love MI, Huber W, Anders S. Moderated estimation of fold change and dispersion for RNA-seq data with DESeq2. *Genome Biol*. 2014;15:550. doi:10.1186/s13059-014-0550-8
23. Stefanova NA, Maksimova KY, Kiseleva E, Rudnitskaya EA, Muraleva NA, Kolosova NG. Melatonin attenuates impairments of structural hippocampal neuroplasticity in OXYS rats during active progression of Alzheimer's disease-like pathology. *J Pineal Res*. 2015;59:163–177. doi:10.1111/jpi.12248
24. Mitsui S, Osako Y, Yokoi F, et al. A mental retardation gene, motopsin/neurotrypsin/prss12, modulates hippocampal function and social interaction. *Eur J Neurosci*. 2009;30:2368–2378. doi:10.1111/j.1460-9568.2009.07029.x
25. Ji H, Ding Z, Hawke D, et al. AKT-dependent phosphorylation of Niban regulates nucleophosmin- and MDM2-mediated p53 stability and cell apoptosis. *EMBO Rep*. 2012;13:554–560. doi:10.1038/embor.2012.53
26. Kamboh MI, Demirci FY, Wang X, et al.; Alzheimer's Disease Neuroimaging Initiative. Genome-wide association study of Alzheimer's disease. *Transl Psychiatry*. 2012;2:e117. doi:10.1038/tp.2012.45
27. Chouraki V, De Bruijn RF, Chapuis J, et al.; Alzheimer's Disease Neuroimaging Initiative. A genome-wide association meta-analysis of plasma Aβ peptides concentrations in the elderly. *Mol Psychiatry*. 2014;19:1326–1335. doi:10.1038/mp.2013.185
28. Bakkour A, Morris JC, Wolk DA, Dickerson BC. The effects of aging and Alzheimer's disease on cerebral cortical anatomy: specificity and differential relationships with cognition. *Neuroimage*. 2013;76:332–344. doi:10.1016/j.neuroimage.2013.02.059
29. Sutherland GT, Janitz M, Kril JJ. Understanding the pathogenesis of Alzheimer's disease: will RNA-Seq realize the promise of transcriptomics? *J Neurochem*. 2011;116:937–946. doi:10.1111/j.1471-4159.2010.07157.x
30. Kolosova NG, Stefanova NA, Korbolina EE, Fursova AZh, Kozhevnikova OS. The senescence-accelerated oxys rats – a genetic model of premature aging and age-dependent degenerative diseases. *Adv Gerontol*. 2014;27:336–340. doi:10.1134/S2079057014040146
31. Mattson MP, Gleichmann M, Cheng A. Mitochondria in neuroplasticity and neurological disorders. *Neuron*. 2008;60:748–766. doi:10.1016/j.neuron.2008.10.010
32. Kolosova NG, Akulov AE, Stefanova NA, et al. Effect of malate on the development of rotenone-induced brain changes in Wistar and OXYS rats: an MRI study. *Dokl Biol Sci*. 2011;437:72–75. doi:10.1134/S0012496611020049
33. Spires-Jones TL, Stoothoff WH, de Calignon A, Jones PB, Hyman BT. Tau pathophysiology in neurodegeneration: a tangled issue. *Trends Neurosci*. 2009;32:150–159. doi:10.1016/j.tins.2008.11.007
34. Mawuenyega KG, Sigurdson W, Ovod V, et al. Decreased clearance of CNS beta-amyloid in Alzheimer's disease. *Science*. 2010;330:1774. doi:10.1126/science.1197623
35. Kanemitsu H, Tomiyama T, Mori H. Human neprilysin is capable of degrading amyloid beta peptide not only in the monomeric form but also the pathological oligomeric form. *Neurosci Lett*. 2003;350:113–116.
36. Kim WR, Sun W. Programmed cell death during postnatal development of the rodent nervous system. *Dev Growth Differ*. 2011;53:225–235. doi:10.1111/j.1440-169X.2010.01226.x
37. Walton NM, Shin R, Tajinda K, et al. Adult neurogenesis transiently generates oxidative stress. *PLoS One*. 2012;7:e35264. doi:10.1371/journal.pone.0035264

38. Loshchenova PS, Sinitsyna OI, Fedoseeva LA, Stefanova NA, Kolosova NG. Influence of antioxidant SkQ1 on accumulation of mitochondrial DNA deletions in the hippocampus of senescence-accelerated OXYS rats. *Biochemistry (Mosc)*. 2015;80:596–603. doi:10.1134/S0006297915050120
39. Kozhevnikova OS, Korbolina EE, Ershov NI, Kolosova NG. Rat retinal transcriptome: effects of aging and AMD-like retinopathy. *Cell Cycle*. 2013;12:1745–1761. doi:10.4161/cc.24825
40. Streit WJ, Braak H, Xue QS, Bechmann I. Dystrophic (senescent) rather than activated microglial cells are associated with tau pathology and likely precede neurodegeneration in Alzheimer's disease. *Acta Neuropathol*. 2009;118:475–485. doi:10.1007/s00401-009-0556-6
41. Markova EV, Obukhova LA, Kolosova NG. Parameters of cell immune response in Wistar and OXYS rats and their behavior in the open field test. *Bull Exp Biol Med*. 2003;136:588–590. doi:10.1023/B:BEBM.0000020212.10768.9a
42. Orlovskaya IA, Toporkova LB, Feofanova NA, Kolosova NG. Peculiarities of bone marrow hemopoiesis in early aging OXYS rats. *Bull Exp Biol Med*. 2007;144:86–88. doi:10.1007/s10517-007-0262-0
43. Obukhova LA, Skulachev VP, Kolosova NG. Mitochondria-targeted antioxidant SkQ1 inhibits age-dependent involution of the thymus in normal and senescence-prone rats. *Aging (Albany NY)*. 2009;1:389–401. doi:10.18632/aging.100043
44. Obukhova LA, Vais VB, Bakeeva LE, Sergeeva SV, Kolosova NG. Structural and functional basis for accelerated thymic involution in OXYS rats. *Adv Gerontol*. 2013;26:229–235. doi:10.1134/S2079057014010081
45. Telegina DV, Kozhevnikova OS, Bayborodin SI, Kolosova NG. Contributions of age-related alterations of the retinal pigment epithelium and of glia to the AMD-like pathology in OXYS rats. *Sci Rep*. 2017;7:41533. doi:10.1038/srep41533
46. Agafonova IG, Kolosova NG, Mishchenko NP, Chaikina EL, Stonik VA. Effect of histochrome on brain vessels and research and exploratory activity of senescence-accelerated OXYS rats. *Bull Exp Biol Med*. 2007;143:467–471. doi:10.1007/s10517-007-0158-z
47. Agafonova IG, Kotelnikov VN, Kolosova NG, Stonik VA. Comparative study on hypertension-induced cerebral vascular alterations in two rat lines. *Appl Magn Reson*. 2012;42:487–497. doi:10.1007/s00723-012-0327-8
48. Pluta R, Furmaga-Jabłońska W, Maciejewski R, Ułamek-Kozioł M, Jabłoński M. Brain ischemia activates β- and γ-secretase cleavage of amyloid precursor protein: significance in sporadic Alzheimer's disease. *Mol Neurobiol*. 2013;47:425–434. doi:10.1007/s12035-012-8360-z
49. Canobbio I, Abubaker AA, Visconte C, Torti M, Pula G. Role of amyloid peptides in vascular dysfunction and platelet dysregulation in Alzheimer's disease. *Front Cell Neurosci*. 2015;9:65. doi:10.3389/fncel.2015.00065